Articles

Study of Phase Selectivity of Organic−Inorganic Hybrid Semiconductors

Chang-Youn Moon,* Gustavo M. Dalpian,† Yong Zhang, and Su-Huai Wei

National Renewable Energy Laboratory, Golden, Colorado 80401

Xiao-Ying Huang and Jing Li

Department of Chemistry and Chemical Biology, Rutgers University, Piscataway, New Jersey 08854

Received February 15, 2006. Revised Manuscript Received April 10, 2006

A new group of hybrid organic−inorganic materials, $A_{II}B_{VI}(en)_{0.5}$ (A = Zn and Cd and B = S, Se, and Te), have been shown to exhibit a number of unusual structurally dependent properties that are not typically found in conventional inorganic and organic materials. However, it is puzzling that for a given inorganic component the hybrid crystal comes in different phases and often favors one over another. Using first-principles methods, we study the structural and electronic properties (e.g., stability and band gap) of the three observed phases: αI, αII, and β. The general chemical trends are revealed and are consistent with experimental observations. A kinetic growth model is proposed to explain the experimental observation of the phase selection for these hybrid materials.

Introduction

Hybrid organic−inorganic semiconductors have attracted significant attention recently owing to their great potential for device applications.[1] These materials combine the strengths of both components: the inorganic part has good electronic properties, and the organic part features ease of assembly. Many of the hybrid materials are assemblies of organic−inorganic nanostructures, which are bonded together through van der Waals interactions or hydrogen bonds.[2] Recently, a new group of II−VI-based hybrid materials, $A_{II}B_{VI}(en)_{0.5}$ (A = Zn, Cd; B = S, Se, Te; en = ethylenediamine), has been synthesized,[3−5] in which the hybrid nanostructures are interconnected through covalent bonds, forming 3D superlattice structures. In contrast to most other hybrid materials, this new group of hybrids shows improved robustness and long-range order, i.e., they exist as fully ordered single crystals with translational symmetry. Furthermore, a number of unusual and potentially useful physical properties have been revealed for a few prototype structures, such as $ZnSe(en)_{0.5}$ and $ZnTe(en)_{0.5}$.[4−9]

$A_{II}B_{VI}(en)_{0.5}$ constitutes inorganic II−VI slabs interconnected by the organic molecules en, resembling ultrashort-period superlattices. These materials have been obtained in either the so-called α or β phases. The α phase has an orthorhombic *Pbca* space group with 64 atoms in the unit cell (8 A, 8 B, 8 N, 8 C, and 32 H). Two types of the α phase (denoted αI and αII in this paper) have been observed.[5] Both α phases have the same space group but differ in the relative position between two neighboring honeycomb-like inorganic layers and the conformation of the organic molecules (TTT−en for αI and GTG′−en for αII; for various conformations of the free en molecule, see ref 10). The β phase, with the en molecule in the TTT conformation, has an orthorhombic *Pnnm* symmetry and a smaller unit cell, with 32 atoms (4 A, 4 B, 4 N, 4 C, and 16 H).[3] Figure 1 shows the crystal structures of the three phases: Parts a and b of Figure 1 are for the αI structure viewed in different directions, parts c and d of Figure 1 are for the αII structure, and parts e and f of Figure 1 are for the β phase. The unit cell and lattice vectors for these structures are also shown in these figures. It is interesting to notice that the inorganic slab in the α phases resembles a twisted wurtzite (WZ) $(11\bar{2}0)$ slab, whereas in the β phase, it resembles a zinc blende (ZB) (110) slab. Experimentally, it is found that the

* Corresponding author. E-mail: Chang_Youn_Moon@nrel.gov.
† Present address: University of Texas, Austin, TX 78712.

(1) *Handbook of Organic−Inorganic Hybrid Materials and Nanocomposites*; Nalwa, H. S., Ed.; American Scientific Publishers: 2003.
(2) Mitzi, D. B. In *Progress in Inorganic Chemistry*; Karlin, K. D., Ed.; John Wiley & Sons: 1999; p 1.
(3) Huang, X.-Y.; Li, J.; Fu, H.-X. *J. Am. Chem. Soc.* **2000**, *122*, 8789−8790.
(4) Huang, X.-Y.; Li, J.; Zhang, Y.; Mascarenhas, A. *J. Am. Chem. Soc.* **2003**, *125*, 7049−7055.
(5) Deng, Z.-X.; Li, L.; Li, Y. *Inorg. Chem.* **2003**, *42*, 2331−2341.
(6) Heulings, H. R., IV; Huang, X.-Y.; Li, J.; Yuen, T.; Lin, C. L. *Nano Lett.* **2001**, *1*, 521−525.
(7) Fu, H.-X.; Li, J. *J. Chem. Phys.* **2004**, *120*, 6721−6725.
(8) Fluegel, B.; Zhang, Y.; Mascarenhas, A.; Huang, X.-Y.; Li, J. *Phys. Rev. B* **2005**, *70*, 205308.
(9) Zhang, Y.; Dalpian, G. M.; Fluegel, B.; Wei, S.-H.; Mascarenhas, A.; Huang, X.-Y.; Li, J.; Wang, L.-W. *Phys. Rev. Lett.* **2006**, *96*, 026405.
(10) Carvalho, L. A. E.; Lourenco, L. E.; Marques, M. P. M. *J. Mol. Struct.* **1999**, *482−483*, 639−646.

10.1021/cm0603811 CCC: $33.50
Published on Web 05/12/2006

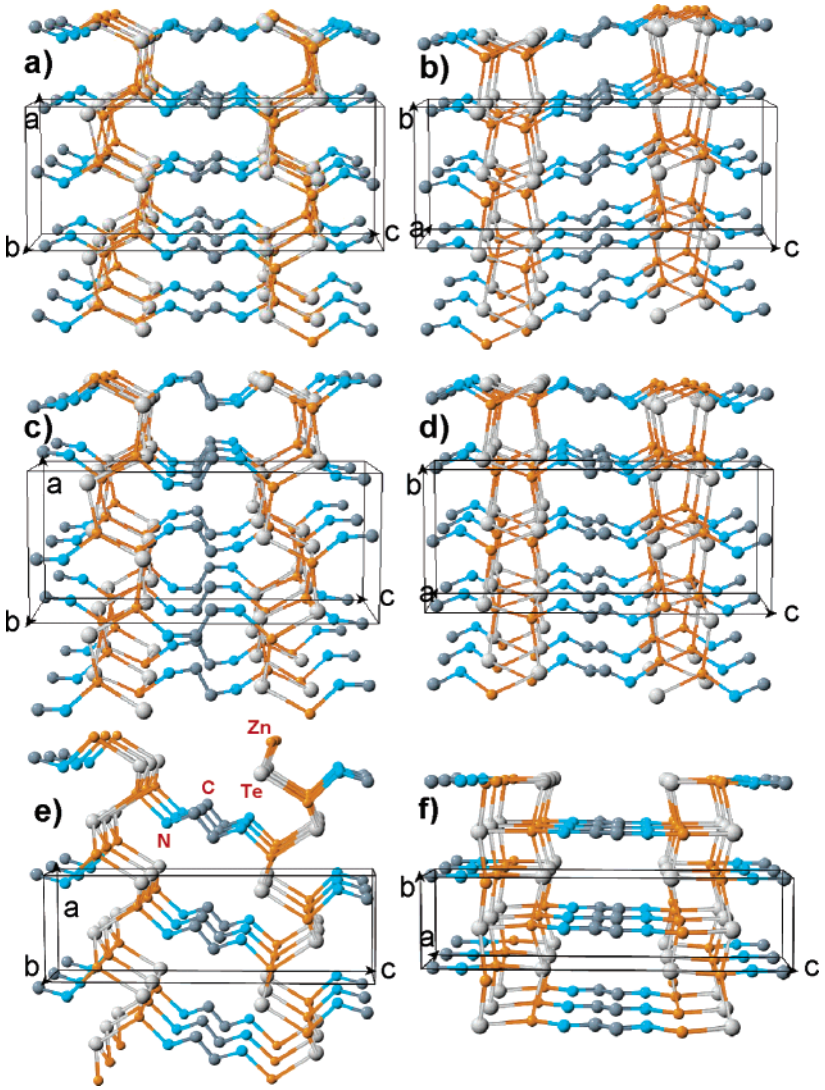

Figure 1. Theoretically calculated structures for the αI-[ZnTe(en)$_{0.5}$] (a and b), αII-[ZnTe(en)$_{0.5}$] (c and d), and β-[ZnTe(en)$_{0.5}$] (e and f) phases of the hybrid along different orientations. The lattice vectors of the unit cells of each structure are also shown. The *c* axis is aligned with the superlattice stacking direction for all structures. For clarity, hydrogen atoms are not shown.

$ZnB_{VI}(en)_{0.5}$ systems prefer to be in the αI phase,[4] whereas $CdB_{VI}(en)_{0.5}$ systems prefer to be in the αII phase.[5] The β phase has been observed only in ZnTe(en)$_{0.5}$.[3] Despite several experimental investigations, it remains a puzzle why these hybrid materials prefer to exist in these different phases. It is also unclear whether the experimentally observed phases are due to the kinetic effects, that is, their formation depends on the growth conditions, or if they are determined by their ground-state total energies. A detailed understanding of the differences among these phases is important, because experimentally it is observed that the hybrids in these different phases have different physical properties (e.g., the α phase of ZnTe(en)$_{0.5}$ has a larger band gap than that of β-ZnTe(en)$_{0.5}$).[4] Therefore, to fine-tune the properties of these hybrid materials and provide guidance for the experimental synthesis effort, it is crucial to understand the relative stability among these different phases.

In this work, we perform a systematic study on the band gap, total energy, and structural properties of $A_{II}B_{VI}(en)_{0.5}$ hybrid materials in the three different phases. Using first-principles calculations, we find that the direct band gap of these hybrid materials in the α phase is larger than that in the β phase, in agreement with experiment.[4] At low temperature, all the materials are more stable in the αI phase, and the stability decreases from β to αII phases. However, the total energy differences among them decrease when the lattice parameter of the corresponding II−VI binary compound increases from ZnS to CdTe. We analyze the stability by considering the individual contributions to the total energy from the organic and inorganic parts and the binding between them. We find that the relative stability of a hybrid material with different phases is determined mainly by the interaction in the organic part. Based on our total energy calculations, we suggest that the experimentally observed metastable αII phase for the Cd hybrids[4,5] could be due to its low-temperature growth conditions.

Computational Details

The calculations were performed using an ab initio plane wave basis code,[11] based on the density functional theory and using ultrasoft pseudopotentials[12] within the generalized gradient ap-

(11) URL http://cms.mpi.univie.ac.at/vasp.
(12) Vanderbilt, D. *Phys. Rev. B* **1990**, *41*, 7892−7895.

Table 1. Calculated Structural Parameters and Band Gap Differences for the Hybrid Materials[a]

inorganic slab	phase	a_0 (ZB) (Å)	calculated lattice parameter (Å)			$\Delta E_{\alpha I-\beta}$ (eV)	$\Delta E_{\alpha I-\alpha II}$ (eV)	$\Delta E^{gap}_{\alpha I-\beta}$ (eV)	$\Delta E^{gap}_{\alpha I-\alpha II}$ (eV)
			a	*b*	*c*				
ZnS	αI	5.449	6.490	6.270	17.287				
			(6.393)	(6.205)	(17.263)[b]				
	αII	(5.405)	6.597	6.275	16.421	−0.338	−0.432	0.185	−0.109
	β		5.160	3.943	17.073				
ZnSe	αI	5.734	6.728	6.548	17.494				
			(6.633)	(6.463)	(17.354)[c]				
	αII	(5.667)	6.892	6.555	16.477	−0.216	−0.371	0.273	−0.097
	β		5.386	4.107	17.211				
ZnTe	αI	6.183	7.230	7.023	17.715				
			(7.061)	(6.927)	(17.524)[d]				
	αII	(6.088)	7.340	6.995	16.766	−0.101	−0.300	0.327	−0.096
	β		5.751	4.397	17.368				
			(5.660)	(4.336)	(17.156)[d]				
CdS	αI	5.929	6.786	6.661	18.101				
	αII	(5.848)	6.961	6.685	16.911	−0.145	−0.267	0.263	0.013
			(6.841)	(6.548)	(16.659)[e]				
	β		5.433	4.240	17.723				
CdSe	αI	6.199	7.025	6.932	18.238				
	αII	(6.077)	7.212	6.926	16.967	−0.096	−0.278	0.296	−0.035
			(7.085)	(6.786)	(16.694)[e]				
	β		5.596	4.400	17.986				
CdTe	αI	6.620	7.470	7.384	18.411				
	αII	(6.460)	7.659	7.345	17.230	−0.066	−0.240	0.344	−0.051
			(7.484)	(7.204)	(16.821)[e]				
	β		5.987	4.665	18.038				

[a] $\Delta E_{\alpha I-\beta}$ and $\Delta E_{\alpha I-\alpha II}$ are the total energy difference (per 64-atom cell) between the αI, αII, and *β* phases. $\Delta E^{gap}_{\alpha I-\beta}$ and $\Delta E^{gap}_{\alpha I-\alpha II}$ are the corresponding band gap energy differences at the Γ point. The numbers in parentheses are the available experimental data (refs 3, 5, 15, 16) at room temperature. For comparison, we also list the calculated and experimental (in parentheses) lattice constants a_0 (ref 17) of the II−VI binary compounds in the ZB structure. [b] Ref 15. [c] Ref 16. [d] Ref 3. [e] Ref 5.

proximation (GGA).[13] All the structural degrees of freedom (lattice parameters and atomic positions) are optimized by minimizing quantum mechanical forces and total energy until the forces in each atom are smaller than 0.02 eV/Å. A plane wave expansion of 435 eV was used in all the calculations. The Brillouin zone integration is performed using the Monkhost−Pack special *k*-points scheme[14] with a mesh of 4 × 4 × 1 for the structural relaxation and 5 × 5 × 3 for final total energy calculations of the optimized structures.

Results and Discussion

The optimized lattice parameters of all the studied materials are compiled in Table 1, which shows good agreement with experimental data.[3,5,15−17] The lattice parameters in the *a* and *b* directions are related to the inorganic slabs, and in the *c* direction it is related to the stacking direction of the superlattice, as shown in Figure 1. The in-plane lattice parameters in the *a* and *b* directions are closely related to the lattice parameter of the II−VI binary compounds. (In the α phase, $ab \approx \sqrt{3}a_{WZ}c_{WZ}$, where a_{WZ} and $c_{WZ} \approx \sqrt{(8/3)}a_{WZ}$ are the lattice parameters of the WZ compounds; in the *β* phase, $ab \approx a_{ZB}a_{ZB}/\sqrt{2}$, where a_{ZB} is the cubic lattice constant and $a_{WZ} \approx a_{ZB}/\sqrt{2}$.) They increase almost monotonically as a_0 increases. We find that the *b* direction typically exhibits minimal distortion compared to that in the II−VI binary material. On the other hand, although the lattice parameter in the *c* direction increases as the anion atomic size increases, the *c* parameters for the Cd system are much larger than those for the Zn system. For example, ZnTe and CdSe have a similar ZB lattice constant, so the *b* parameters of [ZnTe(en)$_{0.5}$] and [CdSe(en)$_{0.5}$] are also similar to each other (Table 1), but the *c* parameter of αI-[ZnTe(en)$_{0.5}$] (17.715 Å) is much smaller than that of αI-[CdSe(en)$_{0.5}$] (18.238 Å). This can be explained by the fact that the connection between the organic/inorganic regions is through the cation−N bond. Because the Cd−N bond length (2.391 Å for αI-[CdSe(en)$_{0.5}$]) is much larger than that of the Zn−N bond (2.137 Å for αI-[ZnTe(en)$_{0.5}$]), the *c* lattice parameters of the Cd hybrids are much larger than those of Zn hybrids.

Another interesting observation is that for the same material, the *c* lattice parameter of the αII phase is much smaller than that of the αI phase. This could be understood by noticing that in the αII phase, the inorganic slab is connected by the GTG′−en, whereas in the αI phase it is connected by the TTT−en. In Figure 2, we show the two conformations of an en molecule. The difference between the two is the orientation of the hydrogen atoms and the lone-pair orbitals of the two nitrogen atoms at both ends of the molecule with respect to the N−C−C−N frame. In the TTT conformation which has a C_{2h} symmetry (Figure 2a), the lone-pair orbital of each nitrogen lies in the N−C−C−N molecular plane, whereas for GTG′ conformation (Figure 2b), which has C_i symmetry, the lone pair points out of the plane. As a consequence, the en molecule and two cation atoms bonded to it are in the same plane for the αI and *β* phases, but the two cation atoms lie off the plane defined by the en

(13) Perdew, J. P.; Chevary, J. A.; Vosko, S. H.; Jackson, K. A.; Perderson, M. R.; Singh, D. J.; Fiolhais, C. *Phys. Rev. B* **1992**, *46*, 6671−6687.
(14) Monkhorst, H. J.; Pack, J. D. *Phys. Rev. B* **1976**, *13*, 5188−5192.
(15) Ouyang, X.; Tsai, T.-Y.; Chen, D.-H.; Huang, Q.-J.; Cheng, W.-H.; Clearfield, A. *Chem. Comm.* **2003**, 886−887.
(16) Huang, X.-Y.; Heulings, H. R., IV; Le, V.; Li, J. *Chem. Mater.* **2001**, *13*, 3754−3759.
(17) *Semiconductors: Basic Data*, 2nd ed.; Madelung, O., Ed.; Springer: Berlin, 1996.

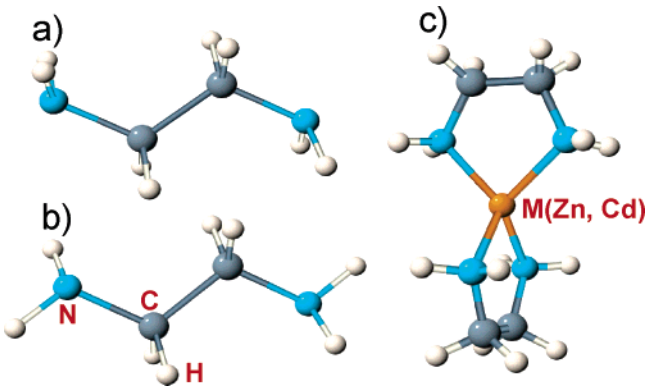

Figure 2. Structures of a free en molecule in (a) TTT and (b) GTG′ conformations. (c) Precursor $[M(en)]^{2+}$ structure formed between cation M (Zn or Cd) and en at room temperature.

molecule for the αII phase (see Figure 1). Because of this difference, the GTG′−en has a smaller length projection along the superlattice direction than the TTT−en, which explains why the αII phase has a much smaller *c* parameter than that of the αI phase. We suggest that this large difference in the *c* parameter can be used as a primary signature to distinguish the αI and αII phases in experimental measurement.

Table 1 also shows the calculated total energy differences among the three phases. We find that (a) the total energy differences are small, on the order of 0.3 eV per 64-atom cell; (b) the total energy for all the hybrid materials studied here follows the same trend, $E(\alpha I) < E(\beta) < E(\alpha II)$, that is, the αI phase is energetically the most stable at low temperature; (c) the total energy differences between the αI and β phases and between the αI and αII phases tend to decrease when the corresponding bulk II−VI binary lattice constant increases. To analyze the trend, we investigate the contributions to the total energy differences from the organic part, and separately the inorganic part, as well as the binding between the two constituents. To find the contribution from the organic part, we remove the II−VI constituent atoms from the supercell of the hybrid, while fixing all the atomic positions of the organic chains inside the supercell, and calculate the total energy, and vice versa for the contribution from the inorganic part. This can be done naturally for these II−VI hybrids because the N lone pair in the en molecule has two electrons and there is no charge at the group II dangling bond in the inorganic slab, so there is no electronic driving force that can cause strong reconstruction in the organic molecule or in the inorganic layers. The total energy differences of the organic part, inorganic part, and the binding energy are shown in Table 2 and are compared with the total energy differences of the hybrids. It is interesting to see that the contributions from the inorganic part and the binding energy part nearly cancel each other; thus, the contribution from the organic part is very similar to the total energy difference. The reason that the energy differences between the αI and β phases ($\Delta E_{\alpha I-\beta}$) are smaller than between the αI and αII phases ($\Delta E_{\alpha I-\alpha II}$) could be understood by noticing that both αI and β phases have the TTT−en conformation, whereas the αII phase has the GTG′−en conformation. Therefore, the energy difference between the αI and β phases reflects mainly the difference of interactions between the en molecules in these two phases. We find that the interaction between the en molecules is less attractive for the β phase, partly because in the β phase the H−H distance between two en molecules is smaller than a critical distance.[18] When the size of inorganic constituent increases, the energy difference decreases due to the reduced coupling between the en molecules. On the other hand, the differences between the αI and αII phases reflect also the difference between the TTT−en and GTG′−en. To verify this, we have calculated the total energy difference of an isolated TTT−en and GTG′−en. We find that the energy of the isolated TTT−en is only about 0.04 eV per molecule lower than that of isolated GTG′−en. However, relative to the free en molecules, there is a considerably larger strain for GTG′−en in the αII phase than TTT−en in the αI phase. Hence, the energy difference of the organic part between the αI and αII phases is mainly determined by the difference of strain on the en molecule in the hybrids.

Table 2. Calculated Energy Differences among the αI, αII, and β Phases for Selected Hybrid Materials[a]

inorganic slab		organic part	inorganic part	binding energy	total
ZnS	$\Delta E_{\alpha I-\beta}$	−0.309	−0.480	0.451	−0.338
	$\Delta E_{\alpha I-\alpha II}$	−0.458	−0.249	0.275	−0.432
ZnTe	$\Delta E_{\alpha I-\beta}$	−0.097	−0.153	0.149	−0.101
	$\Delta E_{\alpha I-\alpha II}$	−0.212	−0.229	0.141	−0.300
CdTe	$\Delta E_{\alpha I-\beta}$	−0.065	−0.158	0.157	−0.066
	$\Delta E_{\alpha I-\alpha II}$	−0.111	−0.161	0.032	−0.240

[a] The total energies are given in eV per 64-atom cell. The total energy difference is the sum of the differences of the organic part energy, the inorganic part energy, and the binding energy.

The other contributions to the energy differences are due to the strain in the inorganic layer and the binding between organic and inorganic layers. We find that in all cases, the bond angle centered at the cation site in the inorganic layer of the αI phase is closer to 120°, whereas for the β phase it is closer to the ideal tetrahedral bond angle of 109.5°. This is consistent with our observation that the αI phase is more stable when the cation is three-fold-coordinated in the sp^2 configuration, such as in the isolated layer, but the binding energy is larger for the β phase when the inorganic layer is connected to the N of the en molecule, forming a four-fold-coordinated sp^3 bond. This explains why the energy differences due to the strain in the inorganic layer and the binding between organic and inorganic layers nearly cancel each other.

Our observation that $A_{II}B_{VI}(en)_{0.5}$ hybrids with large anion atoms are more likely to have different phases because of the reduced energy difference is consistent with experimental observation that only $ZnTe(en)_{0.5}$ is observed to have both αI and β phases.[3] The formation of αI $ZnB_{VI}(en)_{0.5}$ is also consistent with our calculation that the αI phase has the lowest energy. However, ref 5 found that $CdB_{VI}(en)_{0.5}$ forms the αII phases, which, according to our calculation, has the highest energy among the three phases, although the energy differences are relatively small. This suggests that the structure formed during growth may depend sensitively on

(18) Novoa, J. J.; Whangbo, M.-H.; Williams, J. M. *J. Chem. Phys.* **1991**, *94*, 4835−4841.

the specific solutions and growth paths of the synthesis, i.e., kinetics may play an important role in determining the final structure. Indeed, several experimental groups[19−22] have reported that depending on the source reactants, stoichiometric condition, and reaction temperature, etc., one can grow various II−VI inorganic nanostructures with either WZ or ZB phases or different morphologies using the solvothermal method with en as solvent. In the meantime, the relative stability of $A_{II}B_{VI}(en)_{0.5}$ hybrids, which are considered as the intermediate precursors for the formation of II−VI inorganic nanocrystals, as a function of growth parameters has not been systematically investigated. It is likely that the specific phase of the hybrids available so far was also determined by the specific experimental growth conditions. To support this kinetic argument, we have noticed that experimentally it is found that the cation−en complex $[M(en)]^{2+}$ (Figure 2c) precursor forms first at the room temperature,[19,20] and the hybrid or inorganic nanostructure starts to form only after the temperature is increased. Because the Zn−N bond is much stronger than the Cd−N bond, higher growth temperature is required to break the N−cation bond in $[Zn(en)]^{2+}$ than in $[Cd(en)]^{2+}$. Indeed the reaction temperature for Zn hybrids is reported to be about 200 °C, whereas it is about 100 °C for Cd hybrids. After the N−cation bond breaking, the N−C and C−C bonds in the en molecule will rotate, first reaching the GTG′−en conformation and then the TTT−en conformation. However, we find from a nudged elastic band method calculation[23] that there is an energy barrier of about 0.2 eV between the GTG′−en and TTT−en. If the growth temperature is not high enough, the en molecule could remain in the GTG′ conformation, and after the incorporation of the anion atoms to form the hybrids, the final product should be the αII phase. Only after the growth temperature is further increased can the system reach its ground-state phase, i.e., the αI phase with the TTT−en component. This observation may explain why Zn hybrids growing at relatively high temperature are found to be in the most stable αI phase, whereas for Cd hybrids grown at lower temperature, only the αII phase is observed. It also implies that if Cd hybrids could be grown at higher temperature, both αI and β phases may exist, especially for $CdTe(en)_{0.5}$. Likewise, if Zn hybrids could be synthesized at lower temperature, it might be possible to obtain in the αII phase.

Conclusions

In summary, we have studied systematically the electronic, structural, and total energy differences of the hybrid $A_{II}B_{VI}(en)_{0.5}$ system using a first-principles method. We show that the αI phase is the most stable phase for all the hybrids considered, while the relative stability of the αII and β phases increases as the lattice constant of the hybrid increases. The relative stability between the different phases depends mostly on the strain in the organic part of the hybrids and the repulsive H−H interaction between molecules. We also demonstrate the importance of the kinetic effect in determining the phase of the hybrid in actual synthesis and suggest possible synthesis approaches for obtaining the missing phases of these hybrids.

Acknowledgment. The work at NREL is funded by the U.S. Department of Energy, Office of Science, Basic Energy Sciences, under Contract No. DE-AC36-99GO10337 to NREL and an NREL DDRD. The work at Rutgers is supported by NSF (DMR-0422932).

CM0603811

(19) Li, Y.; Liao, H.; Ding, Y.; Qian, Y.; Yang, L.; Zhou, G. *Chem. Mater.* **1998**, *10*, 2301−2303.
(20) Li, Y.; Liao, H.; Ding, Y.; Fan, Y.; Zhang, Y.; Qian, Y. *Inorg. Chem.* **1999**, *38*, 1382−1387.
(21) Liu, Y.; Xu, Y.; Li, J.-P.; Zhang, B.; Wu, D.; Sun, Y.-H. *Chem. Lett.* **2004**, *33*, 1162−1163.
(22) Li, J.; Hong, X.; Li, D.; Zhao, K.; Wang, L.; Wang, H.; Du, Z.; Li, J.; Bai, Y.; Li, T. *Chem. Commun.* **2004**, 1740−1741.
(23) Henkelman, G.; Jonsson, H. *J. Chem. Phys.* **2000**, *113*, 9978−9985.